Label-Free Optical Biochemical Sensor Realized by a Novel Low-Cost Bulk-Silicon based CMOS-Compatible 3-Dimensional Optoelectronic IC (OEIC) Platform

Junfeng Song,[1,2] Xianshu Luo,[1] Jack Sheng Kee,[1] Chao Li[1] and Guo-Qiang Lo[1]

[1]Institute of Microelectronics, A*STAR (Agency for Science, Technology and Research)
11 Science Park Road, Singapore Science Park II, Singapore 117685
[2]State Key Laboratory on Integrated opto-electronics, College of Electronic Science and Engineering,
Jilin University, Changchun, People's Republic of China, 130012
Email: songjf@ime.a-star.edu.sg; Tel: 65-6770-5756, Fax: +65 6773 1914

Abstract

We proposed and demonstrated label-free optical biochemical sensor realized on a novel bulk silicon-based platform with three-dimensional (3D) monolithic optoelectronic integration circuit (OEIC). The Ge-photodetector (Ge-PD) is integrated on bulk-silicon. Optical functional components are built with CMOS back-end-of-line (BEOL). Via this platform, the label-free optical biochemical sensor can get rid of the expensive SOI wafer. The costly tunable laser-source can be replaced by low cost wide-band light source. Optical signal is converted into electrical signal and read out by on-chip Ge-PD directly. This platform facilitates the development of cost-effective portable point-of-care (POC) diagnostic tool. Meanwhile, this also opens up new ways of electronic and photonic devices monolithically integration in 3D.

Introduction

Label-free optical biochemical sensor is testing refractive index changing by optical method (1). It is essential in the applications of medical diagnosis, healthcare and environmental monitoring. This is due to its merits of non-physical contact, high stability, high-speed detection, and high resolution, etc. Previously, we have developed a new electrical-tracing assisted optical biochemical sensing structure, which is monolithically integrated with multiple OEIC components on a single SOI chip (2-4). Such as grating coupler, thermal optical controlled tunable filter, label-free optical biochemical sensor and Ge-PD are integrated together. It has greatly reduced testing cost and seems suitable with POC request. However, it still has some of issues. For instance, SOI wafer is 10× costly than bulk-silicon. Silicon microring is with small size but the sensitivity not high. The buried oxide of SOI impedes heat-dissipation, which will made bad impact for electrical devices.

To overcome those issues, in this work, we propose a bulk-silicon based 3D-OEIC platform. Electrical devices can be fabricated on bulk-silicon. All optical devices use deposited materials and fabricated by BEOL process. This platform has, in addition to the aforementioned advantages of wafer cost and BOX issues, some other advantages: 1) Optical devices can be made with low-index contrasting material which has higher optical sensivity; 2) Different wavelength range can be selected, unlike SOI in which optical wavelength must be longer than 1.1 µm; and 3) Combining the advantages of existing electrical IC- and optical IC- technology.

Label-Free Optical Biochemical Sensor by Bulk-Si based 3D-OEIC Platform

A. Bulk-Si Based 3D-OEIC PD Structure

The basic concept of general SOI-based evanescent-coupled PD structure and the proposed bulk-Si based 3D-OEIC PD structure are illustrated in Fig. 1. The conventional silicon waveguide is replaced by PECVD SiN waveguide (core ~400 ×1000 nm^2). A scattering grating sits at the end of waveguide for vertical light coupling into the underneath Ge-PD. An Al mirror is designed on top of the scattering grating as a reflector to enhance the Ge-PD to collect light more efficiently. Detailed fabrication process is as described in (5). The Ge-PD is simply formed as P-i-N junction. For characterization purpose, the bulk-Si based 3D-OEIC Ge-PD is incorporated with a Y-branch, as shown in Fig. 2(a). Fig. 2(b) shows the zoom-in top view of the PD. Al mirror and electrodes are with same first metal layer. Fig. 2(c) shows the X-SEM for region along the scattering grating. Fig. 2(d) shows the SEM structure of the scattering grating of SiN. Ge-PD I-V characteristics with different optical input power are shown in Fig. 3(a). We can get the responsivity is ~0.2 A/W at 1550 nm. Fig. 3(b) shows the extracted responsivity at different reverse biased voltages and wavelengths. Shorter wavelength is with higher responsivity. Fig. 3(c) shows the dynamic response of PD at reverse bias of 5 V. 3-dB bandwidth is only 2 GHz. However, by means of Trans-Impedance Amplifier (TIA) and higher reverse bias (10 V), we can achieve 20 Gb/s data rate (see inset).

B. Bulk-Si Based 3D-OEIC Label-Free Optical Biochemical Sensor Structure.

In this study, we utilize this new platform for the application of label-free optical biochemical sensor. For cost saving benefit, we replace the SOI by bulk-Si wafer, and thus the typical Si waveguide is replaced by SiN based waveguide which has higher sensitivity as well. The schematics of device structure are shown in Fig. 4(a) and 4(b) for top and cross-section views, respectively. It consists of the basic building elements of coupler, tunable filter, sensor and PD. Coupler is made of 1D grating and a underneath metal mirror. The use of metal mirror is to enhance the light coupling efficiency. Tunable filter is made of an add/drop micro-ring resonator (MRR) with a heater above it. Using SiN waveguide along with thermo-optical effect, heater can modify the oscillation wavelength. Then simply, the sensor is just an exposed add/drop MRR. Lastly, the PD is 3D-OEIC Ge-PD described in Section (A).

C. Bulk-Si Based 3D-OEIC Label-Free Optical Biochemical Sensor Fabrication Process

The fabrication started with 8-inch bulk-silicon wafer. First, the wafer is pre-cleaned, followed with the epitaxial of 1 μm blank Ge deposition. To increase the electrical field in the intrinsic Ge region to increase the PD response speed, we etch away the P- and N- type regions with 400 nm step height. The implantations are performed with 45˚ tilting angle and 90˚ rotation angles, to ensure the doping species being well implanted into the waveguide sidewall. Following annealing of 500°C for 30s, 400 nm SiO_2 layer is deposited. With the contact holes formation, a metal stack of 25 nm TaN/750 nm AlSiCu/50 nm TaN is deposited and patterned as the first metal layer. Subsequently, another 4.5 μm oxide layer is deposited to clad between the Ge layer and metal layer, followed by chemical-mechanical planarization (CMP) to planarize the surface. SiN of 450nm was then deposited by low-temperature PECVD (400˚C), followed by CMP again. SiN~400nm is remained after the planarization. SiN waveguide is then patterned, along with 2 μm SiO_2 deposition on top. Then 5 nm Ti/150 nm TiN are deposited as the heating element. After heater patterning, 600 nm SiO_2 is deposited and CMP planarization is repeated. After opening via holes to contact to heater and to the first metal layer, 2 μm AlSiCu is deposited as the top metal. With top metal patterning, a thick SiO_2 is deposited and planarized with CMP. The following steps are bond pad opening, sensing windows opening and local thermal trench patterning. The subsequent steps are dicing, micro-fluidic packaging to complete the sample preparation before testing.

D. Demonstration of Bulk-Si Based 3D-OEIC Label-Free Biochemical Sensor

As comparisons with Fig. 4(a) and (b), Fig. 4(c)-4(k) describe the top and cross-section of SEM pictures for each building element. The cross-section position is showed by red dished line in top SEM pictures. Fig. 5(a)-5(d) show the fabricated bio-chip, the chip-PCB wire-bonded system with microfluidic packaging, the testing setup and final prototype. Fig. 6 shows the bottom Al mirror reduced ~1-4dB of loss of SiN grating couplers. Fig. 7 shows the spectrum of tunable filter (with tracing ring) and it's FSR in top and bottom, respectively. FSR determines the incident light useful spectrum range. Fig. 8 shows incident light spectrum and tracing ring through port spectrum. The tracing ring regulation ability, sensing ring sensitivity and system resolution determine total system detection limit. Fig. 9 shows tracing ring regulation ability is ~16.5 nm/W. Adopt the undercut technique, the regulation ability can be improve 20-ford (3,4). Fig. 10 shows sensing ring with sensitivity of 166.5 nm/RIU, which suggests ~2-3× higher than that of using Si-microring (2). Fig. 11 shows the resolution of $R=3\sigma=57.4$ μW. Fig. 12's top figure shows the sensing performance of the proposed 3D-OIEC biochemical sensor by scanning the heater voltage and recorded photo current response. Different powers are applied to thermally tune the microring in order to trace the resonance shift induced due to the solution refractive index change, which is summarized in bottom of Fig. 12. The bulk resolution sensing sensitivity is $S\approx7.9$ W/RIU. Therefore, the detection limit is estimated $DL=R/S\approx7.3$ μRIU. Fig. 13 shows the PD response for different PSS/PAH bi-layer periods. The operation processing is as same as (2). The fitting results show 24.5 mW heater powers for a bi-layer period. Therefore, the surface mass sensitive is $S\approx12.3$ mW/ng·mm^{-2} and detection limit is $DL\approx4.7$ pg·mm^{-2}. This system also can apply into continuously monitoring biochemical reactions. Fig. 14 shows the dynamic behavior of PSS/PAH deposition on the sensing ring surface.

Conclusion

We proposed a 3D monolithic OEIC integration platform on bulk-silicon, and applied for biochemical sensor as a case study. The bulk solution detection limit of ~7.3 μRIU and surface mass detection limit of 4.7 pg·mm^{-2} are achieved. Such bulk-Si based 3D-OEIC platform technology can also apply into on-chip optical interconnection.

Acknowledgments

This work was supported by the Science and Engineering Research Council of A*STAR (Agency for Science, Technology and Research), Singapore. First author is also partially supported by National Natural Science Foundation of China (NSFC, Grant No. 61177090, 61377048).

References

(1) X. Fan, I. M. White, S. I. Shopova, H. Zhu, J. D. Suter and Y. Sun, "Sensitive optical biosensors for unlabeled targets: A review," *Anal. Chim. Aata*, 620(1), 2008, 8-26.
(2) J. Song, X. Luo, X. Tu, M. K. Park, J. S. Kee, H. Zhang, M. Yu, G. Q. Lo and D. L. Kwong, "Electrical tracing-assisted dual-microring label-free optical bio/chemical sensors," *Opt. Express*, 20(4), 4189-4197, 2012
(3) J. Song, X. Luo, J. S. Kee, K. Han, C. Li, M. K. Park, X. Tu, H. Zhang, Q. Fang and L. Jia, "Silicon-based optoelectronic integrated circuit for label-free bio/chemical sensor," *Opt. Express*, 21(15), 2013, 17931-17940.
(4) J. F. Song, X. S. Luo, J. S. Kee, Q. Liu, K. W. Kim, Y. Shin, M. K. Park, K. W. Ang, and G. Q. Lo, "A Novel Optical Multiplexed, Label-Free Bio-Photonic-Sensor Realized on CMOS-Compatible OEIC Platform," in *IEDM Tech. Dig.*, 2013, 381-384.
(5) J. F. Song, X. Luo, X. Tu, L. Jia, Q. Fang, T.-Y. Liow, M. Yu and G. Q. Lo, "Three-dimensional (3d) monolithically integrated photodetector and WDM receiver based on bulk silicon wafer," *Opt. Express*, 22(16), 2014, 19546-19554.

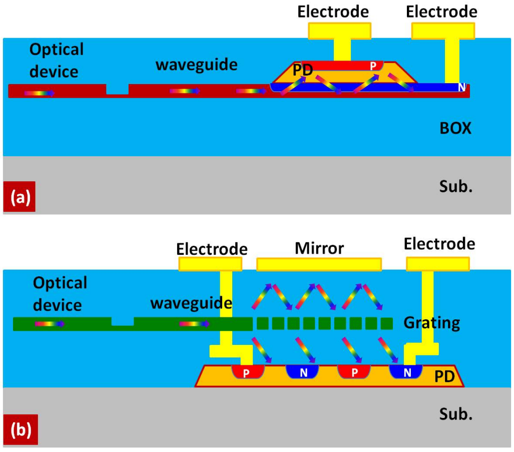

Fig. 1 Schematic illustrations. (a) The SOI-based PD. Optical and electrical devices are in same silicon film. (b) The proposed bulk Si-based 3D PD. Optical devices and electrical devices are separate up and down. A metal mirror is enhanced light collection for PD.

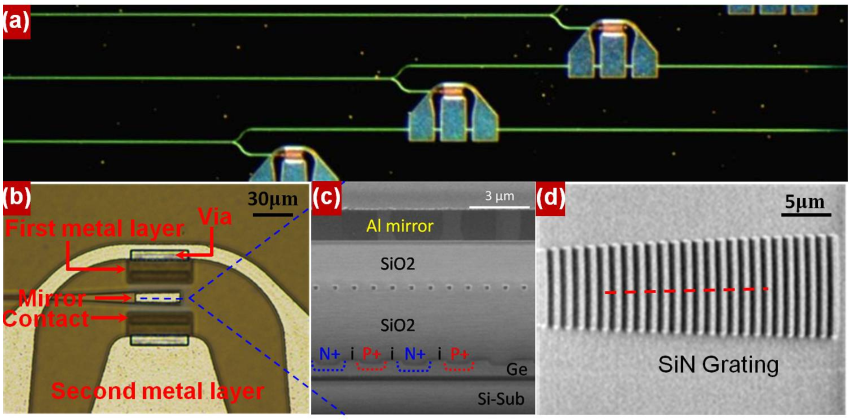

Fig. 2 (a) is optical microscope picture of the Y-branch integrated with a 3D PD. (b) is zoom-in of top view of 3D PD. (c) is the cross-sectional SEM image of the Ge PD region. Bottom is Ge film with interleaved P-i-N junction. The thickness of SiO_2 between SiN grating and Ge is 4 μm. Cladding SiO_2 is ~3μm. A 2μm Al mirror is on the top of SiN scattering grating. (d) is the top view SEM picture of the SiN scattering grating. Grating is with period of 1.1μm.

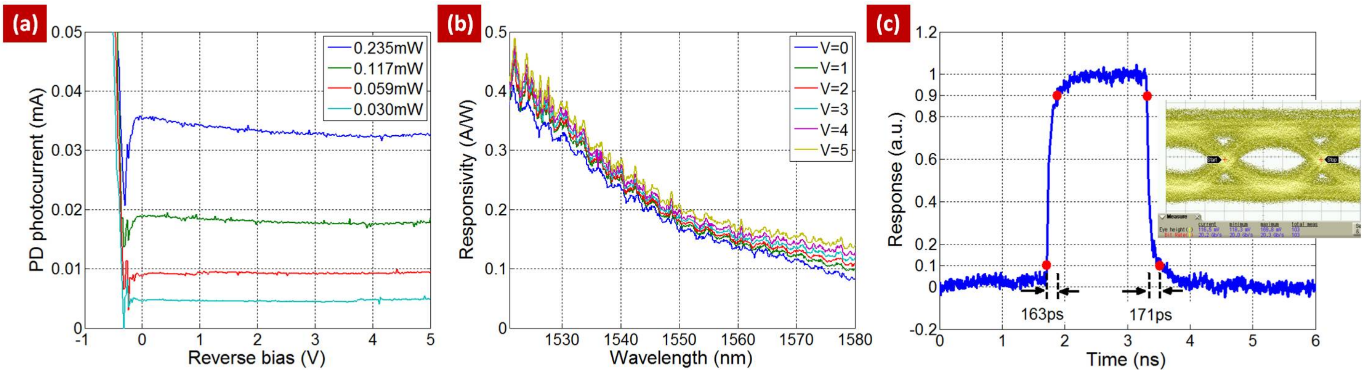

Fig. 3. Characteristics of 3D-PD. (a) The PD photocurrent with different optical input power. Laser wavelength is 1550nm. PD length is 48μm. (b) The PD responsivity vs. wavelength for different reverse bias. (c) PD dynamic response under optical square wave with 5V reverses bias. Rise time and fall time is 163ps and 171ps respectively. A 20Gb/s eye diagram with 10V reverse bias is inserted.

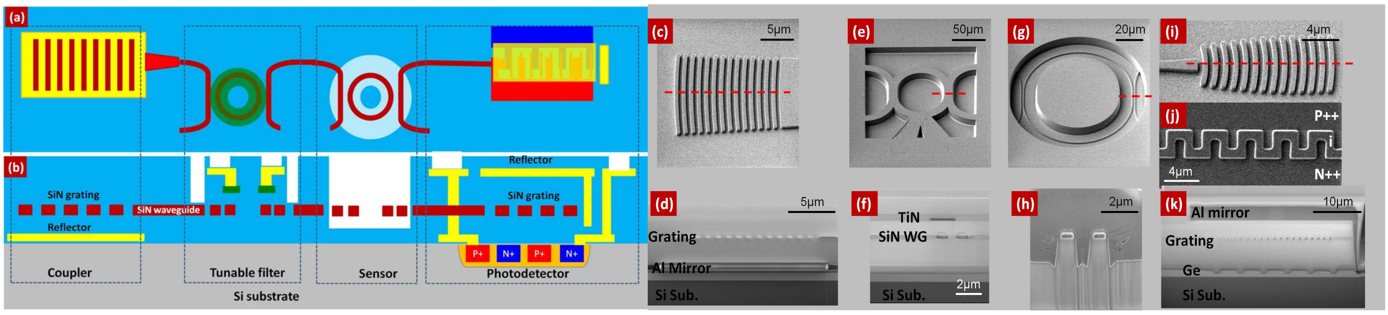

Fig. 4. Schematic illustrate map of 3D bulk-Si OEIC biochemical sensor system. (a) is top view and (b) is cross section view. (c) SEM image of vertical grating coupler. Period is 1.1μm and duty ratio is 50%. (d) Cross section of vertical grating coupler with an Al mirror underneath. The distance of grating and Al mirror is ~ 4μm. (e) Thermal tunable filter (tracing ring) with heat isolation trench. (f) Cross section SEM image of heater (TiN), microring resonator and waveguide coupler. The distance of TiN and SiN waveguide are 2μm. The thickness of TiN is 120nm. Gap of waveguide is 700nm. (g) Sensing microring resonator with opening window. The sensing microring is racetrack type. Radius is 40 μm and the length of straight waveguide coupler is 20μm. (h) Cross section of sensing ring waveguide with coupling waveguide. (i) SiN scattering grating. (j) Ge interleaved P-i-N junction. The width of intrinsic Ge is 1μm. (k) Cross section of photodetector, SiN grating, Ge interleaver P-i-N junction and Al mirror. The distance between grating and Ge film is ~5μm, Al mirror and grating is 2.5μm.

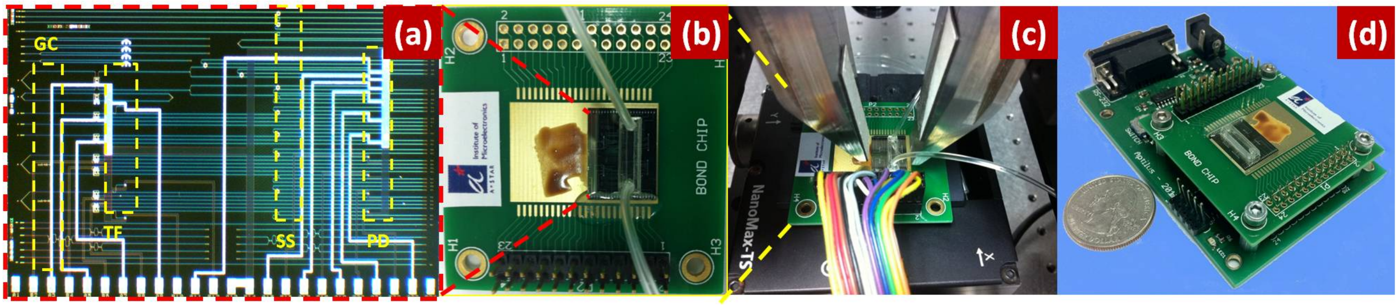

Fig. 5. (a) Microscope description of sensor chip. Yellow dished box denotes the grating coupler (GC), tunable filter (TF), sensor microring (SS) and PD. (b) Microscope of after wire bonding and Microfluidic packaging. (c) Testing setup. (d) Fully packaged Prototype in reference with a quarter coins. Overall size is < 6 cm^2 ×10 cm^2.

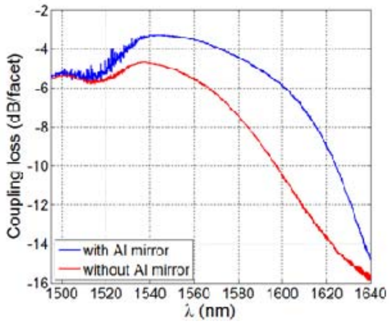

Fig. 6. Vertical grating coupler loss vs. wavelength. The blue color curve is with Al mirror underneath, and red color curve is without Al mirror.

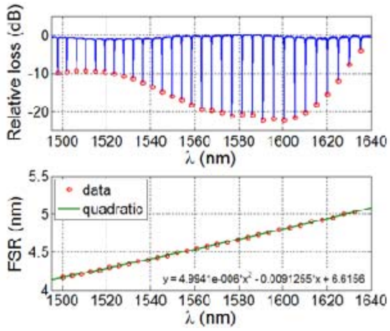

Fig. 7. Top shows spectrum of tracing ring. The transmission loss is balanced by reference waveguide. Bottom figure is FSR with wavelength.

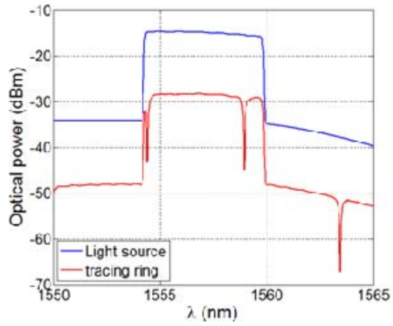

Fig. 8. According to FSR of Fig. 7. The input light spectrum width is set as ~5.1 nm that showed by blue curve. As comparison, tracing ring spectrum is shown as red color curve.

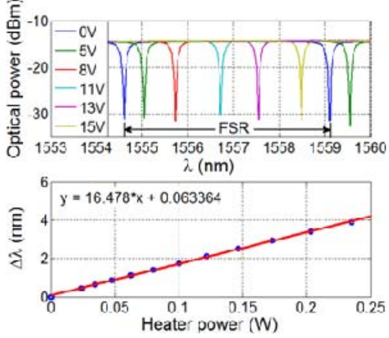

Fig. 9. Top figure shows the spectrum of tunable filter ring (tracing ring) with different heater bias. Bottom shows the resonance wavelength shift with heater power.

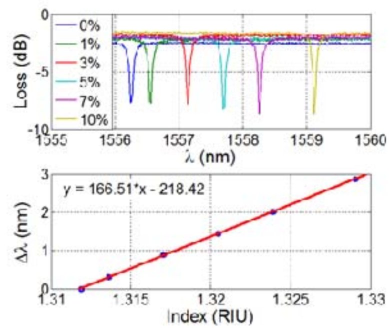

Fig. 10. Top figure shows spectrum of sensing ring with different concentration of NaCl solution. Bottom figure shows the resonance wavelength shift with refractive index of NaCl

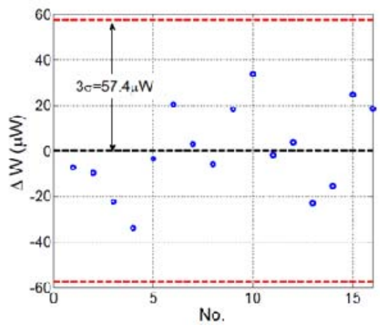

Fig. 11. Fitted electrical power centre shift of each measurement. σ is standard deviation and 3σ is resolution.

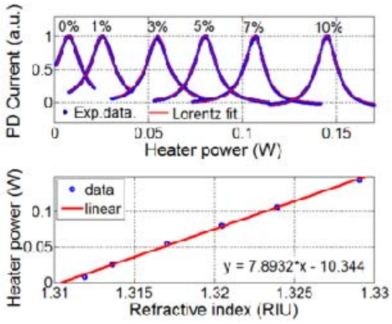

Fig. 12. Top shows PD current in response to heater power for different NaCl concentration. Dots are experimental results. Red color curves are Lorentz fitted. Bottom figure shows the optical reflect index of solution vs. heater power. Blue circles denote peak electrical power, and red color line is a linear fitted curve.

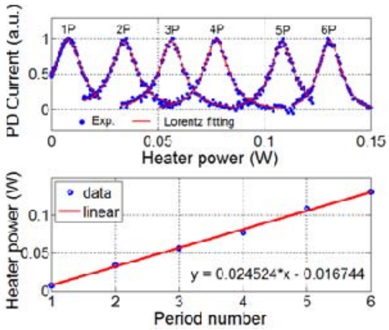

Fig. 13. Top figure shows the PD response for different number of PAH/PSS bi-layer periods. Blue dots are experimental data and red curves are Lorentz fitting results. Bottom figure is linear fitting results.

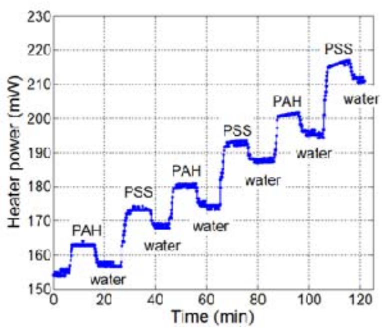

Fig. 14. Dynamic response of PAH and PSS deposition process. A single data point takes ~9 sec. Every step duration is ~10 minutes.